The following supplements accompany the article

Understanding the 3D environment of pelagic predators from multidisciplinary oceanographic surveys to advance ecosystem-based monitoring

Maite Louzao*, Isabel García-Barón, Anna Rubio, Udane Martínez, José Antonio Vázquez, José Luis Murcia, Enrique Nogueira, Guillermo Boyra

*Corresponding author: maite.louzao@gmail.com

Marine Ecology Progress Series doi.org/10.3354/meps12838

Supplement 1. Non-breeding diet of pelagic seabirds

Table S1.1. Non-breeding diet of highly pelagic seabirds in the Northwest Atlantic Ocean extracted from Ronconi et al. (2010).

Species	n	Krill	Herring	Squid	Mackerel	Sandlance	Pollock livers
Great shearwater	**231**	**0.19**	**0.36**	**0.135**	**0.105**	**0.125**	**0.08**
Sooty shearwater	**22**	**0.265**	**0.305**	**0.17**	**0.065**	**0.13**	**0.05**

Supplement 2. Horizontal fields of oceanographic descriptors

To obtain horizontal fields of temperature (TEM, ºC), salinity (SAL, p.s.u.), dynamic height (DYN), depth of maximum temperature gradient (DTG, m) and maximum temperature gradient (MTG, ºC m^{-1}), we used the Optimal Statistical Interpolation (OSI) scheme described in Gomis et al. (2001) in a regular 33 × 54 grid, covering all the study area with regular node distances of 0.15º × 0.15º. Since this scheme analyses observation increments (Gomis et al. 2001), we used a local 1st order degree polynomial least-square fit to the observations to estimate a background field and to compute the anomalies. Then, a Gaussian function for the correlation model between observations (assuming 2D isotropy) was set up, with a correlation length scale of 25-km, chosen according to DYN profiles correlation statistics obtained at different depths. The noise-to-signal (NTS) variance ratio used for the analysis of TEM, SAL and DYN were: 0.005, 0.05, and 0.01, respectively. This ratio was defined as the variance of the observational error divided by the variance of the interpolated field (the latter referring to the deviations between observations and the mean field). This parameter allows the inclusion in the analysis an estimation of the observational error and adjustments of the weight of the observations on the analysis (the larger the NTS parameter, the smaller the influence of the observation). Finally, all fields were spatially smoothed, with an additional low-pass filter with a cut-off length scale of 30 km, in order to avoid aliasing errors due to unresolved structures.

After station DYN data were interpolated onto the grid, all levels were referred to the lowest one by adding the contributions of all the levels below. This method allows profiles obtained at shallow stations take part in the recovery of the dynamic height field and has been previously tested over the continental shelf (e.g. Rubio et al. 2009). Then, geostrophic velocities (GEO, m s^{-1}) were obtained by the first derivative between adjacent grid nodes of the DYN interpolated fields.

The used of in situ CTD data can be challenging and different methodological steps are necessary to undertake to assure the validity of the oceanographic outcomes used to describe the regional of

oceanography. Among them, the OSI is a robust methodology to obtain interpolated fields from uneven spaced data (Torres et al. 2011, León et al. 2015, Cotroneo et al. 2016). In the schema used here, too additional parameters control the scales that are resolved and permit to filter out small structures that could emerge from the interpolation and that are not resolved by the original data. Those are the correlation length scale (which avoids spurious structures between observational points that are too far away) and the cut-off length scale which smooths the resulting interpolated fields to avoid structures under a given scale which are not resolved by the original observations. The first parameter is fixed taking into account the empirical correlation scales computed using the original data. The second one is fixed taking into account the mean distance between CTD stations.

In addition to using a robust methodology, we carefully processed the CTD data to avoid salinity spikes (and the associated density), bias in temperature or conductivity between the profiles of the two ships, low synoptic measurements in a given area, among others. Moreover, resulting OSI fields have been validated individually by comparison with satellite imagery (SST, IR) and Sea Level Anomaly (SLA) maps, and even with the fields from Copernicus CMEMS GLORYS reanalyses.

An example is given in Fig. S2.1 where there is an agreement in the area covered by CTD measurements of the in-situ dynamic heights with the corresponding SLA fields. Satellite SLA fields offer much lower spatial resolution. Satellite SLA can be used as an alternative to obtain dynamic heights in an area where there is no in-situ observational data. SLA mapped fields consist in an optimal interpolation (similar methodology to the one used in this study) of along-track SLA data obtained from a constellation of altimeters onboard satellites measuring the global sea level with a revisit period higher than a week and a track distance around tens of kilometers. Thus, even if the along-track resolution is classically of around 7 km the resulting interpolated (and smoothed) SLA maps and the derived geostrophic currents are of much less spatio-temporal resolution (see for instance Dussurget et al. 2011) that the one obtained from the analysis of in-situ observations, following the methodology used in this study. Moreover, satellite SLA fields present specific problems in the coastal area, where the sea level measurements have lower quality than in the open ocean.

Figure S2.1 (a) Interpolated fields of dynamic height (values in dynamic meters indicated by the respective color bars) and geostrophic vectors at 10 m obtained from JUVENA 2013 CTD data. (b) Interpolated fields of satellite sea level anomalies (SLA) in cm and geostrophic vectors during 12th September 2013.

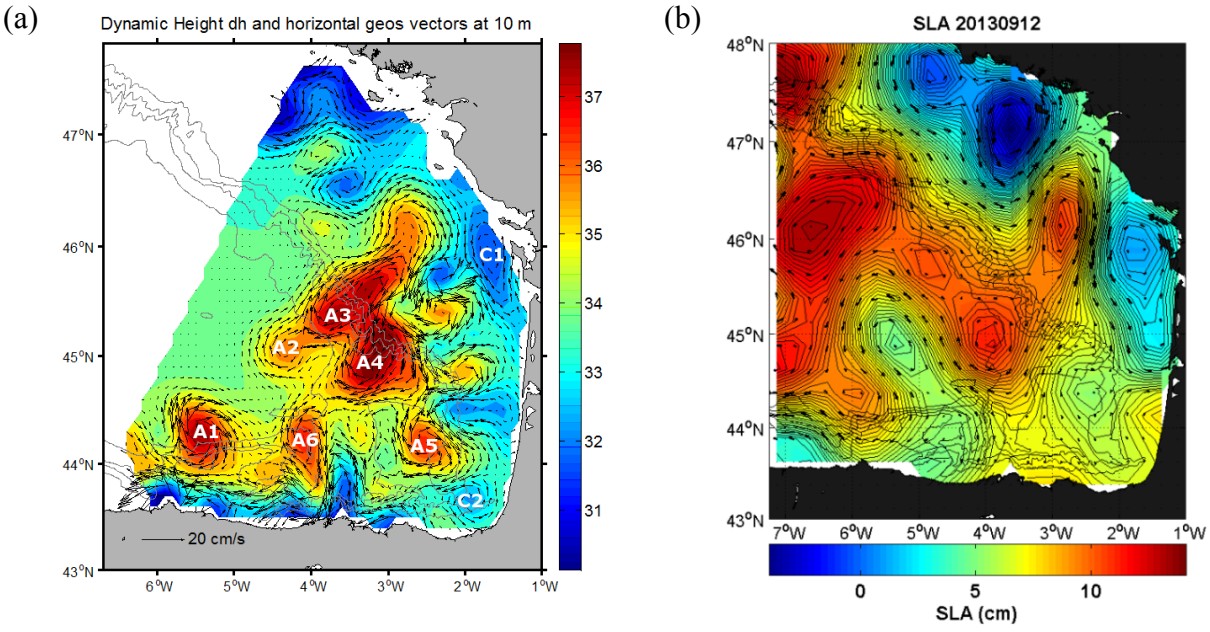

Supplement 3. Static variables

Figure S3.1. Static variables such as (a) bathymetry (BAT, m) and (b) its spatial gradient (BATG), (c) distance to the shelf-break (DSB, km) and distance to the coast (DCO, km).

(a)

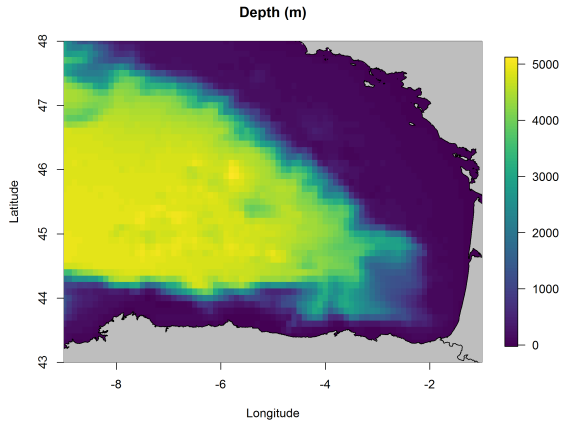

(b)

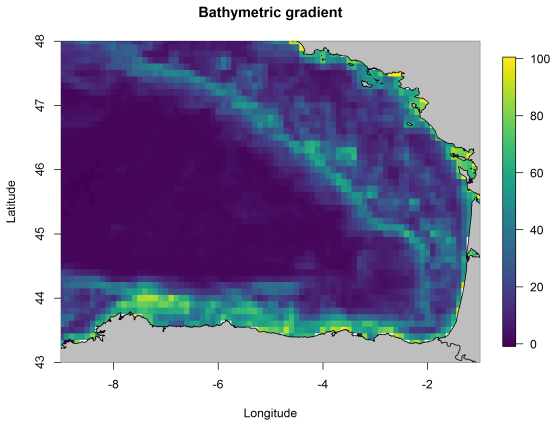

(c)

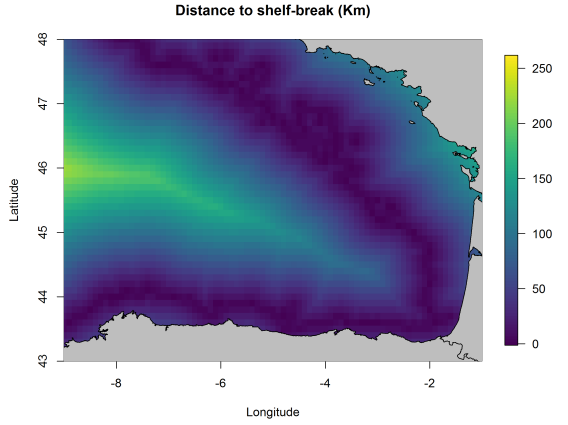

(d)

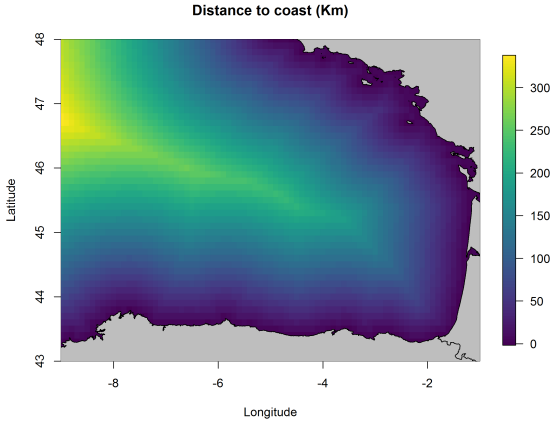

Supplement 4. Characterising the vertical domain

Table S4.1. Summary of pair-wise correlation analysis of preyscapes at different depth ranges by means of Spearman rank correlation coefficients and corresponding significance levels (lower and upper diagonal, respectively). Significance levels were set at <0.05, <0.01 and <0.001; NS: not significant. Strongly correlated (|rs| > 0.5) descriptors are marked in bold. See Table 1 for abbreviations.

	$ANEJ_{10}$	**$ANEA_{10}$**	**PIL_{10}**	**$ANEJ_{DTG}$**	**$ANEA_{DTG}$**	**PIL_{DTG}**	**$ANEJ_{70}$**	**$ANEA_{70}$**	**PIL_{70}**
$ANEJ_{10}$	NA	0.01	0.01	0.001	0.05	0.01	0.001	0.001	NS
$ANEA_{10}$	0.082	NA	0.001	NS	0.001	0.001	NS	0.001	0.001
PIL_{10}	0.094	**0.614**	NA	NS	0.001	0.001	NS	0.001	0.001
$ANEJ_{DTG}$	**0.680**	-0.011	0.05	NA	NS	0.05	0.001	0.01	NS
$ANEA_{DTG}$	0.069	**0.763**	**0.751**	0.038	NA	0.001	NS	0.001	0.001
PIL_{DTG}	0.086	**0.568**	**0.984**	0.066	**0.758**	NA	NS	0.001	0.001
$ANEJ_{70}$	**0.630**	-0.051	-0.029	**0.829**	-0.047	-0.029	NA	NS	NS
$ANEA_{70}$	0.128	**0.541**	**0.826**	0.081	**0.672**	**0.805**	0.040	NA	0.001
PIL_{70}	0.038	**0.537**	**0.727**	0.020	**0.687**	**0.702**	-0.030	**0.746**	NA

Table S4.2. Summary of pair-wise correlation analysis of oceanographic variables at different depth ranges by means of Spearman rank correlation coefficients and corresponding significance levels (lower and upper diagonal, respectively). Significance levels were set at <0.05, <0.01 and <0.001; NS: not significant. Strongly correlated (|rs| > 0.5) descriptors are marked in bold. See Table 1 for abbreviations.

	SAL_{10}	**TEM_{10}**	**GEO_{10}**	**SAL_{DTG}**	**TEM_{DTG}**	**GEO_{DTG}**	**SAL_{70}**	**TEM_{70}**	**GEO_{70}**
SAL_{10}	NA	0.01	0.01	0.01	0.01	0.01	0.01	0.01	NS
TEM_{10}	-0.409	NA	0.01	0.01	0.01	0.01	0.001	0.01	0.01
GEO_{10}	-0.212	0.303	NA	0.01	0.01	0.01	0.001	0.05	0.01
SAL_{DTG}	**0.973**	-0.334	-0.206	NA	0.01	0.01	0.01	0.01	0.01
TEM_{DTG}	-0.394	**0.904**	0.254	-0.355	NA	0.01	0.001	0.01	0.01
GEO_{DTG}	-0.261	0.346	**0.973**	-0.258	0.311	NA	0.001	0.01	0.01
SAL_{70}	**0.627**	-0.019	0.051	**0.643**	-0.020	0.022	NA	0.001	0.01
TEM_{70}	0.361	0.101	-0.088	0.430	0.121	-0.109	0.004	NA	0.01
GEO_{70}	0.066	0.325	**0.630**	0.101	0.288	**0.679**	0.145	0.296	NA

Supplement 5. Seabird detection functions

Table S5.1 Modelling the detection function for sooty shearwaters during the JUVENA surveys. Hn: half-normal. Hr: hazard-rate. Beaufort: sea state. waveH: wave height. Cloud: cloud cover.

Model	Key function	Formula	AIC	Cramér-von Mises p-value	Pa	se(Pa)	ΔAIC
hn	hn	~1	1963.132	0.738	0.489	0.032	0.000
hn.year	hn	~as.factor(Year)	1965.102	0.629	0.482	0.032	1.971
hn.size	hn	~group size	1965.119	0.720	0.489	0.036	1.988
hr	hr	~1	1965.999	0.358	0.603	0.032	2.868
hr.year	hr	~as.factor(Year)	1966.427	0.282	0.604	0.031	3.295
hr.size	hr	~size	1967.638	0.285	0.611	0.032	4.506
hn.beaufort	hn	~as.factor(Beaufort)	1969.324	0.657	0.486	0.033	6.192
hr.beaufort	hr	~as.factor(Beaufort)	1970.053	0.520	0.598	0.032	6.922
hn.waveH	hn	~as.factor(waveH)	1972.434	0.794	0.480	0.033	9.303
hn.cloud	hn	~as.factor(cloud)	1973.665	0.702	0.483	0.033	10.533
hr.waveH	hr	~as.factor(waveH)	1974.887	0.954	0.530	0.045	11.755
hr.cloud	hr	~as.factor(cloud)	1975.842	0.245	0.613	0.030	12.710

Table S5.2. Modelling the detection function for great shearwaters during the JUVENA surveys. Hn: half-normal. Hr: hazard-rate. Beaufort: sea state. waveH: wave height. Cloud: cloud cover.

Model	Key function	Formula	AIC	Cramér-von Mises p-value	Pa	se(Pa)	ΔAIC
hr.beaufort	hr	~as.factor(Beaufort)	6394.602	0.837	0.397	0.027	0.000
hr.year	hr	~as.factor(year)	6396.791	0.841	0.401	0.026	2.189
hr.size	hr	~ group size	6398.656	0.779	0.399	0.027	4.054
hr	hr	~1	6399.875	0.746	0.404	0.026	5.273
hr.waveH	hr	~as.factor(waveH)	6405.030	0.796	0.402	5.239	10.428
hr.cloud	hr	~as.factor(cloud)	6408.496	0.790	0.398	0.026	13.894
hn.beaufort	hn	~as.factor(Beaufort)	6413.327	0.002	0.469	0.017	18.725
hn.year	hn	~as.factor(year)	6415.097	0.002	0.481	0.015	20.495
hn.waveH	hn	~as.factor(waveH)	6417.314	0.005	0.470	5.675	22.712
hn	hn	~1	6422.534	0.001	0.488	0.015	27.932
hn.size	hn	~size	6423.510	0.001	0.487	0.015	28.908
hn.cloud	hn	~as.factor(cloud)	6426.154	0.002	0.482	0.015	31.552

Figure S5.1. (a) The detection function and (b) the quantile-quantile plot of the detection model with the lowest Akaike information criterion (AIC) for sooty shearwaters, as well as (c) the detection function and (d) the quantile-quantile plot for great shearwaters (see Table S5.1 and S5.2, respectively).

(a)

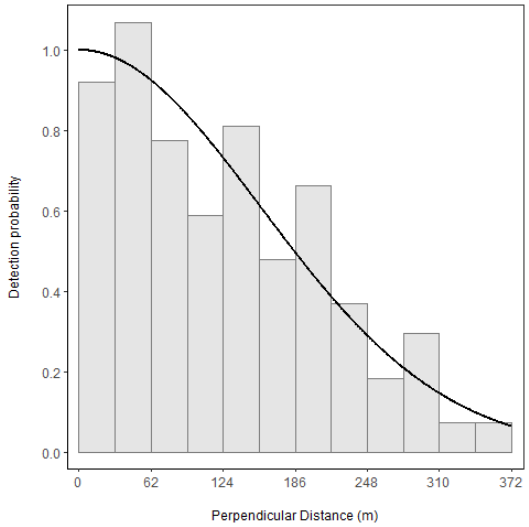

(b)

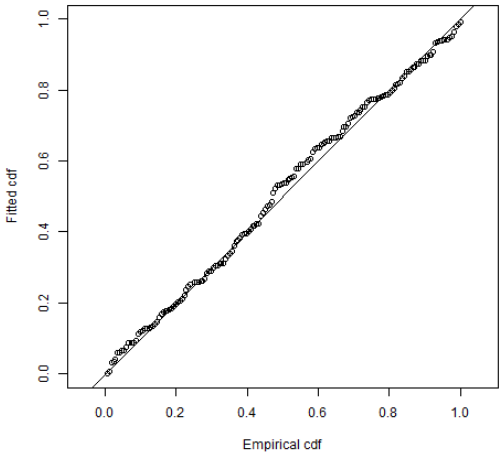

(c)

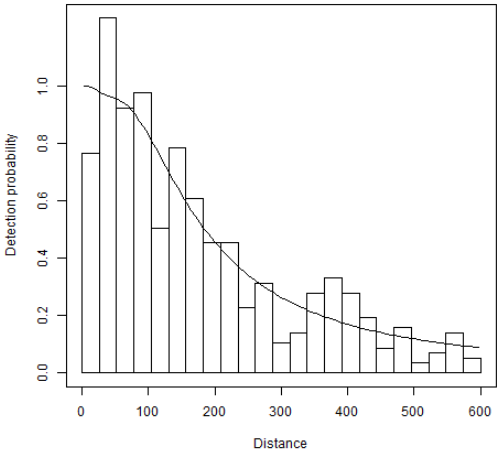

(d)

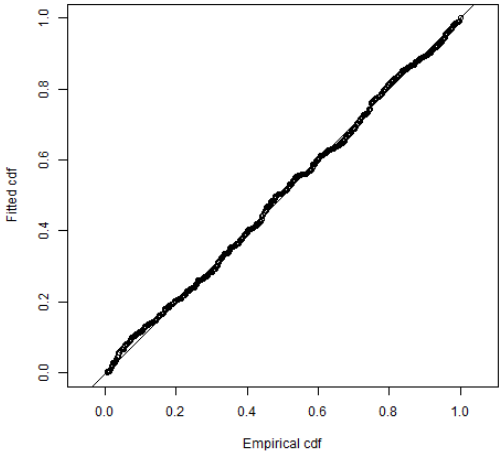

Supplement 6. Correlation between descriptors

Table S6.1. Pair-wise Spearman-rank correlation coefficient and corresponding significance levels (lower and upper diagonal, respectively) between 3D environmental descriptors integrated over the depth of maximum temperature gradient (DTG), 2D environmental descriptors and static descriptors. Significance levels were set at <0.05, <0.01 and <0.001; NS: not significant. Strongly correlated (|rs| > 0.5) descriptors are marked in bold. See Table 1 for abbreviations.

	$ANEJ_{DTG}$	**$ANEA_{DTG}$**	**PIL_{DTG}**	**SAL_{DTG}**	**TEM_{DTG}**	**GEO_{DTG}**	**DTG**	**MTG**	**SSTG**	**BAT**	**BATG**	**DCO**	**distSB**
$ANEJ_{DTG}$	NA	NS	0.05	0.001	0.001	0.001	NS	NS	0.05	0.01	NS	NS	NS
$ANEA_{DTG}$	0.038	NA	0.001	0.05	0.001	NS	NS	NS	0.01	0.001	0.001	0.001	NS
PIL_{DTG}	0.066	**0.758**	NA	0.05	0.001	0.001	NS	NS	NS	0.001	0.001	0.001	0.01
SAL_{DTG}	-0.195	0.078	0.07	NA	0.001	0.001	0.001	0.001	0.01	0.001	NS	NS	NS
TEM_{DTG}	0.131	-0.227	-0.244	-0.354	NA	0.001	0.001	NS	NS	0.001	0.001	0.001	NS
GEO_{DTG}	0.142	-0.056	-0.117	-0.259	0.312	NA	0.001	0.001	0.001	0.05	0.001	NS	0.001
DTG	-0.004	-0.017	-0.010	**0.541**	-0.173	-0.275	NA	0.001	0.001	0.001	0.001	0.001	0.001
MTG	0.013	-0.032	0.037	-0.264	-0.032	-0.131	-0.169	NA	NS	0.001	0.01	NS	0.001
SSTG	-0.064	0.081	-0.009	-0.088	0.013	0.364	-0.365	-0.05	NA	0.001	0.001	0.001	0.001
BAT	0.082	-0.238	-0.267	0.198	0.476	0.074	0.361	-0.199	-0.263	NA	0.001	0.001	0.001
BATG	-0.053	0.158	0.110	-0.035	-0.209	0.129	-0.235	-0.09	0.397	**-0.586**	NA	0.001	0.001
DCO	0.012	-0.239	-0.234	0.054	0.243	-0.029	0.292	-0.053	-0.349	**0.656**	**-0.524**	NA	0.001
DSB	0.045	0.049	0.093	0.051	0.033	-0.181	0.112	0.143	-0.249	0.266	**-0.688**	0.235	NA

Table S6.2. Pair-wise Spearman-rank correlation coefficient and corresponding significance levels (lower and upper diagonal, respectively) between surface 3D environmental descriptors, 2D environmental descriptors and static descriptors. Significance level set at <0.05, <0.01 and <0.001; NS: not significant. Strongly correlated (|rs| > 0.5) descriptors are marked in bold. See Table 1 for abbreviations.

	$ANEJ_{10}$	**$ANEA_{10}$**	**PIL_{10}**	**SAL_{10}**	**TEM_{10}**	**GEO_{10}**	**DTG**	**MTG**	**SSTG**	**BAT**	**BATG**	**DCO**	**DSB**
$ANEJ_{10}$	NA	0.01	0.01	0.001	0.001	0.001	0.001	0.05	0.001	0.01	NS	NS	NS
$ANEA_{10}$	0.082	NA	0.001	NS	0.001	NS	0.001	NS	0.001	0.001	0.001	0.001	NS
PIL_{10}	0.094	**0.614**	NA	NS	0.001	0.01	NS	NS	NS	0.001	0.001	0.001	0.001
SAL_{10}	-0.399	-0.021	0.059	NA	0.001	0.001	0.001	0.001	0.05	0.001	NS	NS	NS
TEM_{10}	0.228	-0.171	-0.236	-0.408	NA	0.001	0.001	0.01	NS	0.001	0.001	0.001	NS
GEO_{10}	0.224	0.025	-0.094	-0.213	0.305	NA	0.001	0.001	0.001	NS	0.001	0.01	0.001
DTG	-0.376	-0.161	-0.055	0.486	-0.193	-0.225	NA	0.001	0.001	0.001	0.001	0.001	0.001
MTG	0.063	0.031	0.048	-0.251	-0.083	-0.166	-0.169	NA	NS	0.001	0.01	NS	0.001
SSTG	0.237	0.166	0.016	-0.065	0.032	0.406	-0.365	-0.05	NA	0.001	0.001	0.001	0.001
BAT	-0.083	-0.292	-0.295	0.139	0.456	0.039	0.361	-0.199	-0.263	NA	0.001	0.001	0.001
BATG	0.026	0.203	0.122	-0.015	-0.166	0.173	-0.235	-0.090	0.397	**-0.586**	NA	0.001	0.001
DCO	-0.029	-0.255	-0.261	0.056	0.176	-0.090	0.292	-0.053	-0.349	**0.656**	**-0.524**	NA	0.001
DSB	0.026	0.018	0.101	0.031	0.023	-0.213	0.112	0.143	-0.249	0.266	**-0.688**	0.235	NA

Supplement 7. Surface environmental conditions

Figure S7.1. 3D preycapes represented by the spatial patterns of log-transformed biomass (tonnes) of juveniles ($ANEJ_{10}$) (a-d) and adults ($ANEA_{10}$) (e-h) of European anchovy and European pilchard ($ANEJ_{10}$) (i-l) at 10 m depth during the 2013-2016 period. White solid and dashed lines depict the annual effort coverage corresponding to the R/V Emma Bardán and R/V Ramón Margalef, respectively. Isobaths of 200 m, 1000 m and 2000 m are outlined. Geographic references are indicated in Figure 1.

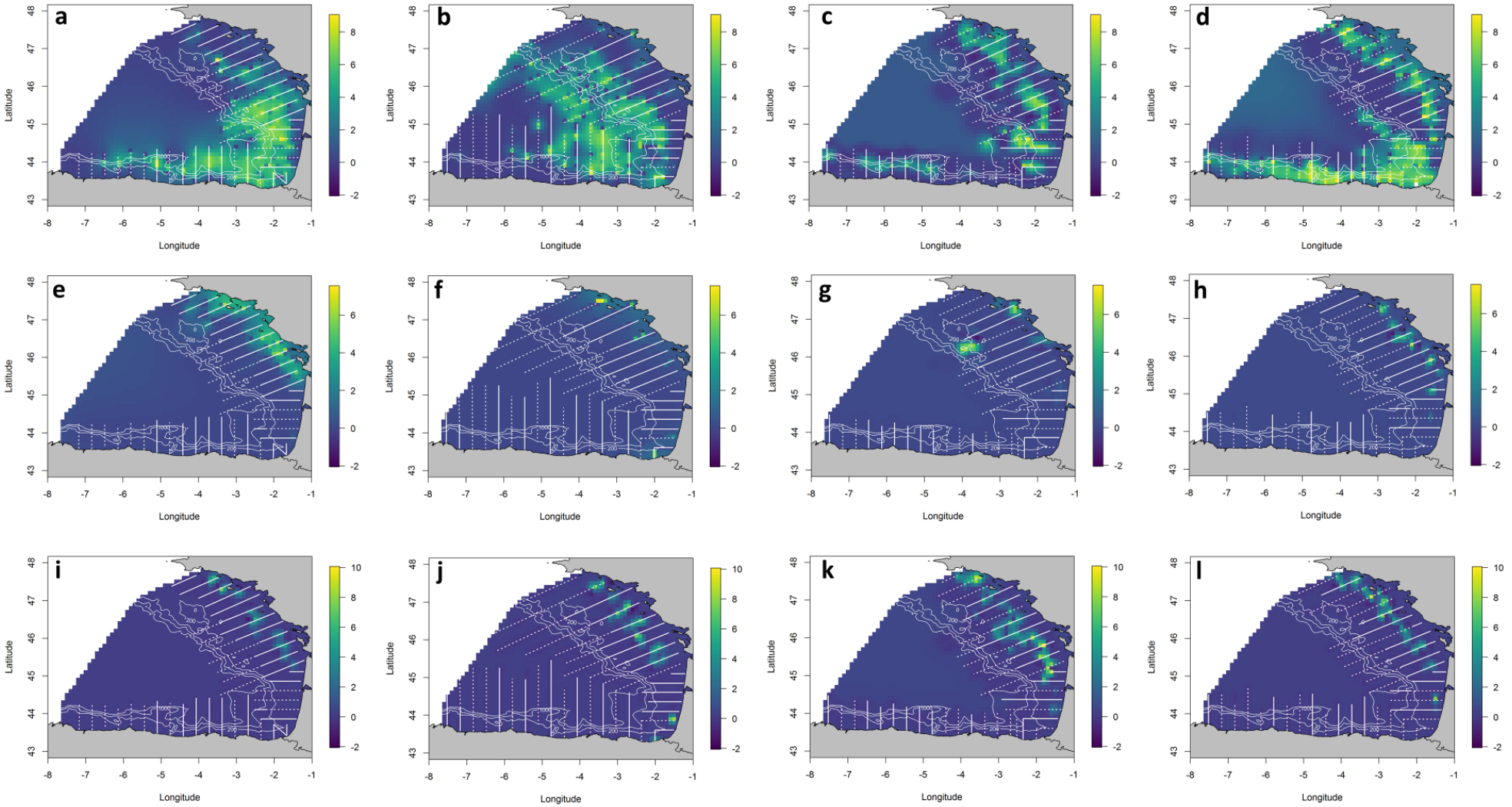

Figure S7.2**.** 3D oceanographic environment represented by median values of (a-d) salinity (values in p.s.u., SAL_{10}), (e-h) temperature (values in ºC, TEM_{10}) and (i-l) geostrophic velocity module (values in ms^{-1}, GEO_{10}) at 10-m depth during the 2013-2016 period. Dots and stars represent CTD cats performed by Emma Bardán and Ramón Margalef RVs, respectively. Isobaths of 200 m, 1000 m and 2000 m are outlined. Geographic references are indicated in Figure 1.

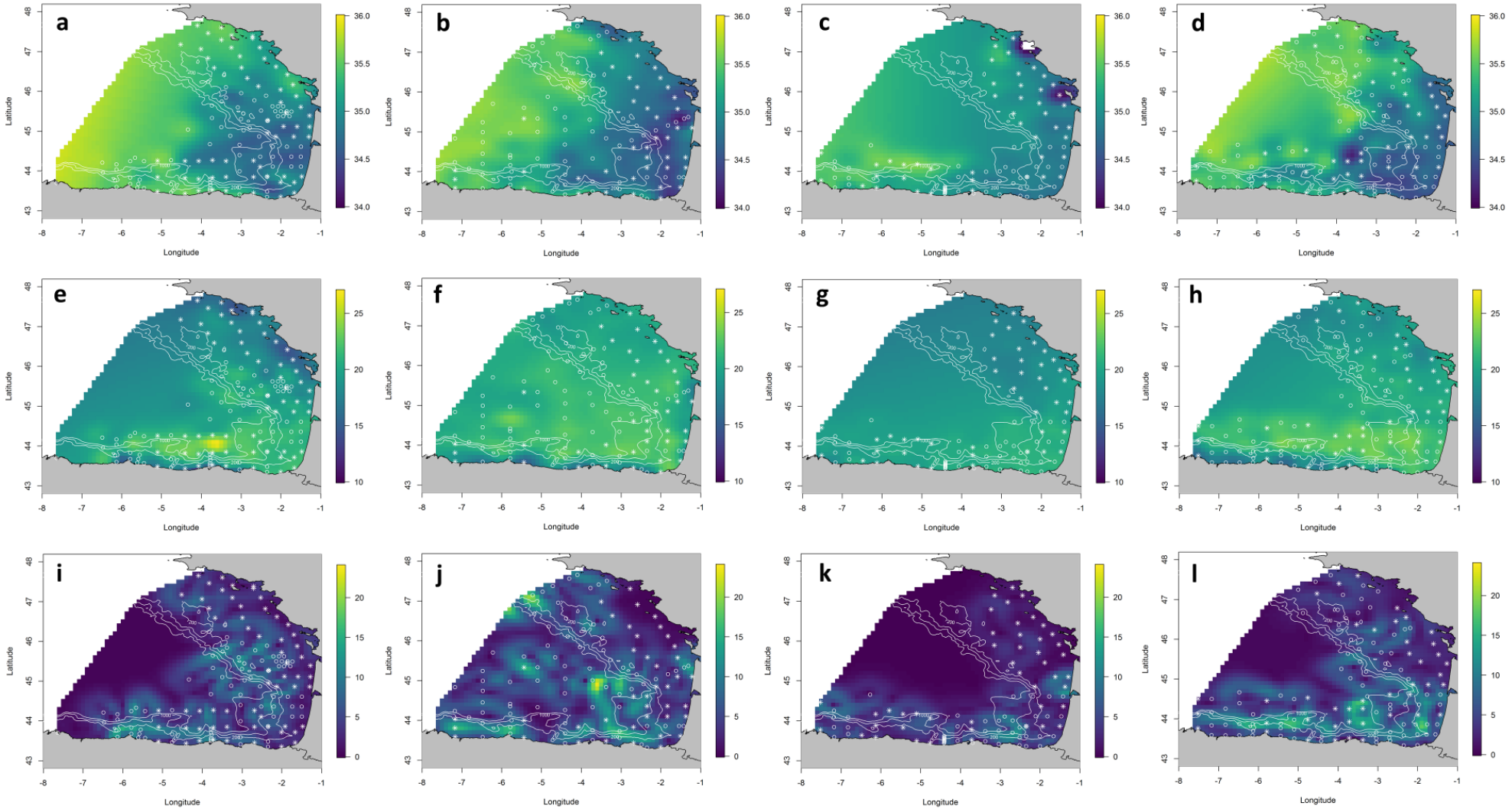

Literature cited

Cotroneo Y, Aulicino G, Ruiz S, Pascual A, Budillon G, Fusco G, Tintoré J (2016) Glider and satellite high resolution monitoring of a mesoscale eddy in the algerian basin: Effects on the mixed layer depth and biochemistry. J Mar Syst 162:73–88 https://doi.org/10.1016/j.jmarsys.2015.12.004

Dussurget R, Birol F, Morrow R, Mey P De (2011) Fine resolution altimetry data for a regional application in the Bay of Biscay. Mar Geod 34:447–476 https://doi.org/10.1080/01490419.2011.584835

Gomis D, Ruiz S, Pedder MA (2001) Diagnostic analysis of the 3D ageostrophic circulation from a multivariate spatial interpolation of CTD and ADCP data. Deep Sea Res Part I 48:269–295 https://doi.org/10.1016/S0967-0637(00)00060-1

León P, Blanco JM, Flexas M del M, Gomis D, Reul A, Rodríguez V, Jiménez-Gómez F, Allen JT, Rodríguez J (2015) Surface mesoscale pico–nanoplankton patterns at the main fronts of the Alboran Sea. J Mar Syst 143:7–23 https://doi.org/10.1016/j.jmarsys.2014.10.010

Ronconi R, Koopman H, McKinstry C, Wong S, Westgate A (2010) Inter-annual variability in diet of non-breeding pelagic seabirds *Puffinus* spp. at migratory staging areas: evidence from stable isotopes and fatty acids. Mar Ecol Prog Ser 419:267–282 https://doi.org/10.3354/meps08860

Torres AP, Reglero P, Balbin R, Urtizberea A, Alemany F (2011) Coexistence of larvae of tuna species and other fish in the surface mixed layer in the NW Mediterranean. J Plankton Res 33:1793–1812 https://doi.org/10.1093/plankt/fbr078